ELSEVIER

LEED and DFT investigation on the (2 × 2)-S overlayer on Co(0001)

J. Lahtinen [a,*], P. Kantola [a], S. Jaatinen [a], K. Habermehl-Cwirzen [a], P. Salo [a],
J. Vuorinen [b], M. Lindroos [b], K. Pussi [c], A.P. Seitsonen [d]

[a] *Laboratory of Physics, Helsinki University of Technology—TKK, P.O. Box 1100, FIN-02015 TKK, Finland*
[b] *Institute of Physics, Tampere University of Technology, P.O. Box 692, FIN-33101 Tampere, Finland*
[c] *Laboratory of Electronics Materials Technology, Lappeenranta University of Technology,*
P.O. Box 20, FIN-53851 Lappeenranta, Finland
[d] *Institute of Mineralogy and Condensed Matter Physics, CNRS and University of Pierre and Marie Curie,*
P.O. Box 115, 75252 Paris cedex 05, France

Abstract

The geometric surface structure of a (2 × 2)-S layer formed by adsorption of hydrogen sulfide at 185 K on the Co(0001) surface has been determined by low energy electron diffraction (LEED) experiments and density-functional theory (DFT) calculations. The favored atomic configuration consists of sulfur atoms residing at the fcc-hollow sites with S–Co distance of 2.2 ± 0.1 Å. Buckling in the first layer is negligible and the three nearest-neighbor Co atoms below the S atom are symmetrically moved by 0.05 ± 0.09 Å along the surface away from the S atom. The DFT calculations confirm the hollow-site adsorption and give further information on the electronic structure of the system.
© 2005 Elsevier B.V. All rights reserved.

1. Introduction

Sulfur adatoms adsorbed on transition metal surfaces form a variety of ordered surface structures. The main motivation to study these structures has been the poisoning of catalysts in the presence of sulfur contamination. Even a small amount of sulfur has been reported to suppress,

---
* Corresponding author. Tel.: +358407487667; fax: +35894513116.
  E-mail addresses: Jouko.Lahtinen@hut.fi (J. Lahtinen), svj@fyslab.hut.fi (S. Jaatinen).

e.g. CO adsorption [1,2], and thus the low S coverage structures can be considered as the most important in respect of catalysis. We have found that sulfur blocks the CO adsorption on Co(0001), one S atom blocking effectively 1.2 CO sites [2], whereas in the case of hydrogen adsorption [3] the blocking is complete.

The lowest sulfur structure exhibiting a long range order on close-packed transition metal surfaces is (2×2). For catalytic purposes the coverage of 1/4 monolayer (ML) is large, but with low energy electron diffraction (LEED) more sparse structures are hard to analyze. The local (2×2) adsorption structure have been resolved on Ru(0001) [4], Re(0001) [5], Ni(111) [6,7] and Pt(111) [8]. The earlier results on close-packed transition metal surfaces indicate that on hcp metals the adsorption site is hcp and with fcc metals the site is fcc. Based on this information we could expect sulfur to adsorb on the Co(0001) surface at the hcp site. On the other hand, we could raise the question whether there is a notable difference in the adsorption energy between the threefold hollow fcc and hcp sites.

In this work, we have studied the local adsorption structure of sulfur forming a (2×2)-S structure on Co(0001) using $I(V)$ LEED measurements combined with TensorLEED and density-functional theory (DFT) calculations. This study continues the analysis of the local adsorption structures on Co(0001) reported earlier for $(\sqrt{3} \times \sqrt{3})R30°$-CO [9], (2×2)-K [10], (2×2)-K + 2CO [11], and $(\sqrt{7} \times \sqrt{7})R19.1°$-C$_6H_6$ [12].

2. LEED experiments and analysis

2.1. LEED experiments

The LEED experiments were performed in a stainless steel UHV chamber with a base pressure of 50 nPa. Beside the LEED system, the apparatus was equipped with facilities for X-ray photoelectron spectroscopy (XPS) and thermal desorption spectroscopy (TDS).

The Co(0001) single crystal specimen was attached to the sample holder by spot welded tantalum wires. The wires were also used for resistive

heating and conducting heat to the heat sink cooled with liquid nitrogen. This setup resulted in a lowest sample temperature of 160 K, as measured by a K-type thermocouple spot-welded to the sample edge. The initial cleaning procedure of the Co(0001) sample featuring repeated sputtering and annealing cycles has been described earlier [13,14].

Before each measurement, the surface residues were removed by 1–2 h Ar$^+$ sputtering, followed by annealing at 650 K for 30 min. After the annealing the sample was cooled down to 220 K. As this took about 15 min, a clean surface was not warranted because of residual gas adsorption. To ensure the cleanliness, the sample was then flashed up to 500 K and cooled again. As the surrounding of the sample was at very low temperature, the second cooling took a negligible amount of time. The cleanliness of the cobalt surface was verified by XPS and using the brightness of the Co(0001) LEED spots. After the second cooling, sulfur was delivered to the surface as hydrogen sulfide at 220 K after which the sample was flashed to 650 K to desorb all the hydrogen.

The amount of sulfur on the surface was measured using XPS before and after the LEED experiments. The 2p XPS signal of S corresponding to the best (2×2)-S LEED pattern was calibrated to sulfur coverage using the TDS yield of hydrogen after H$_2$S exposure and comparing that to the yield after H$_2$ saturation exposure at 180 K from the same surface. This calibration suggested a sulfur coverage around 0.23 ML which is close to the nominal coverage of 0.25 ML. The calibration of the hydrogen yield has been explained in Ref. [3].

The LEED measurements were performed with a four-grid rear-view LEED unit. Normal incidence was attained by visual investigation of the equivalent beams before each measurement and also during the analysis. The $I(V)$ data were recorded at 220 K by a CCD camera attached to the system. During the measurement the acceleration voltage was changed in steps of 2 eV and at each step two pictures from the diffraction pattern were averaged and saved. This procedure resulted in a series of pictures, which were saved and used later to obtain the $I(V)$ curves. More details on the LEED measurement is available in Refs. [9,15].

The diffraction pattern was very stable and no signs of weakening was observed when the pattern was visually inspected before and after the $I(V)$ measurements. To ensure that the radiation damage is negligible, the LEED pictures were recorded sweeping the electron energy first up and then down. These two data sets were then compared, and no changes were observed indicating that no electron beam induced changes during measurements occurred.

The $I(V)$ data consist of seven beams ((1,0), (1,1), (2,0), (1/2,0), (1/2,1/2), (3/2,0), and (1,1/2)) collected at normal incidence with energies between 27 and 503 eV. The cumulative energy range is 1619 eV, of which 971 eV is for integer order beams and 648 eV for fractional order beams.

2.2. LEED analysis

The multilayer relaxation and reconstruction of sulfur-covered cobalt surface has been analyzed using the Symmetrized Automated Tensor LEED package of Barbieri and Van Hove [16]. Prior to the theoretical analysis each beam was individually background corrected by fitting an exponentially increasing function to user's chosen minima. The exponential increase in the background intensity level is caused by the diffraction spots approaching each other when the energy is increased. Symmetrically equivalent beams were then averaged together in order to increase the signal to noise level and compensate for any remaining deviation of the angular alignment.

Theoretical $I(V)$ spectra were calculated in the range from 25 to 510 eV. Phase shifts up to $l_{max} = 14$ were tested to describe the scattering properties of sulfur and cobalt, but the results were obtained using $l_{max} = 11$ giving the same results as with the higher l values. The phase shifts were calculated using Barbieri/Van Hove Phaseshift package [16]. Other non-structural parameters include the Debye temperatures (θ_D) for cobalt (450 K) and sulfur (300 K) and an energy-independent imaginary part of the inner potential (−5.0 eV). The vibrations of atoms were assumed to be isotropic in the analysis and they were represented with the Debye temperatures.

Agreement between the theory and experiment was tested using Pendry R-factor, and the structure with the smallest R-factor was chosen to be the favored structure. Error bars were determined by using sensitivity curves and Pendry's RR-factor [17].

2.3. DFT calculations

First-principles DFT calculations were made for the S on Co(0001) system to verify and analyze the experimental results in this paper. The optimized geometric and electronic structures were obtained by employing self-consistent spin-polarized calculations as implemented in the Vienna Ab initio Simulation Package (VASP) [18–20].

The total energies were calculated using the projector augmented-wave method [21,22] with a cutoff energy of 335 eV and the generalized gradient approximation by Perdew et al. [23] for the exchange-correlation potential. The $8 \times 8 \times 1$ Monkhorst–Pack mesh [24] including the Γ-point was used for the k-point sampling. The positions of the atoms in the system were relaxed until the forces acting on the ions were smaller than about 0.05 eV/Å and the difference between the successive total energy values was less than about 1 meV, corresponding to the accuracy of 0.02 Å in the distances between the atoms. The relative error in the calculated energy values when compared to each other was tested and estimated to be about 0.02 eV with respect to the finite cutoff energy and k-point mesh.

We used a slab including seven atomic Co layers within a (2×2) surface cell and a vacuum region equivalent to five layers or about 10 Å. On the Co(0001) surface we placed an S atom on one side of the slab to study the adsorption corresponding 1/4 ML of S on Co(0001). The adsorption geometries at different adsorption sites were searched allowing all the atoms to relax except for the atoms in the bottom-most Co layer. For a surface system we applied the calculated bulk values $a = 2.490$ Å and $c/a = 1.615$ which are in agreement with the values $a = 2.507$ Å and $c = 4.070$ found in the literature [25], giving $c/a = 1.62$. The latter values were also used in the dynamical LEED analysis.

3. Results

3.1. LEED results

The experimental intensity vs. energy curves for the three integer and four half-order beams are shown in Fig. 1. The beam intensities have been scaled by factors shown in the figure to enable the drawing of the intensities within the same frames.

The calculations were started by testing sulfur atoms on the fcc, hcp, bridge and top sites. In all these structures the substrate was ideally terminated. The non-structural parameters such as the inner potential and Debye temperatures were kept fixed. The search was conducted first by optimizing vertically the S layer and the four topmost Co layers, and then followed by a full 3D optimization of the S layer and the two topmost Co layers. The search results strongly favored the fcc site with the R-factor of 0.16. The best R-factors for

the other adsorption sites were 0.43, 0.39, and 0.35 for the top, hcp, and bridge site, respectively.

In the final search, only the fcc site was considered. From the structural parameters the layer distance between the S and first Co layer and the layer distances between the three topmost Co layers were optimized. The Co atoms beneath the S atom were allowed to move symmetrically both horizontally and vertically. At this point, the inner potential and Debye temperatures were also optimized giving -5.0 eV for the inner potential and 265 K and 293 K for the Debye temperature of sulfur and cobalt, respectively. The final value of the Pendry R-factor was 0.159 and the R-factors corresponding to each beam are shown in Table 1. Fig. 2 shows the optimum values of the structural parameters and their estimated errors calculated based on the Pendry-RR method.

In the final Co(0001)-p(2×2)-S structure the layer distance between the sulfur atom and the topmost Co layer is 1.59 ± 0.06 Å corresponding to the S–Co distance of 2.2 ± 0.1 Å. The first Co–Co interlayer distance is 2.05 ± 0.04 Å, and thus it has slightly relaxed outwards from the bulk value of 2.035 Å. The second interlayer distance of 2.03 ± 0.04 Å equals the value seen with clean Co(0001).

The first Cobalt layer undergoes a minor reconstruction. The three Co-atoms below the S-atom are moved symmetrically by 0.05 ± 0.09 Å away from the fcc-symmetry point. The buckling (d_b) of the first Co layer defined in Fig. 3 is not seen in the LEED analysis. The final structure of the (2×2)-S layer on Co(0001) surface is presented in Fig. 3 and the corresponding values in Table 2.

3.2. DFT results

The DFT calculations were started by the calculation of the clean Co(0001) surface. The relaxations of the first and second interlayer spacing are -3.0% and $+0.8\%$, respectively, in accordance
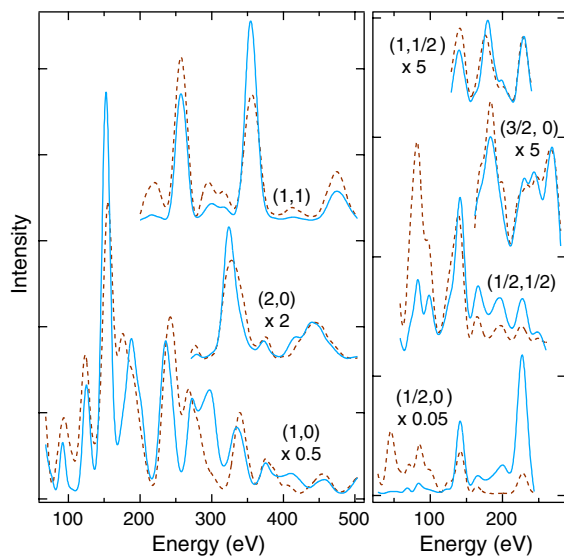

Fig. 1. The measured and calculated $I(V)$ curves. Solid lines represent experimental data and the dashed lines the final Tensor LEED results.

Table 1
The final Pendry R-factors for the different beams of the optimized fcc structure

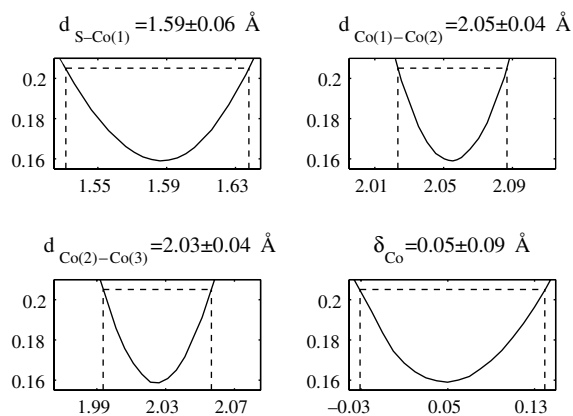| (1,0)	(1,1)	(2,0)	(1/2,0)	(1/2,1/2)	(3/2,0)	(1,1/2)	R_{tot}
0.25	0.07	0.17	0.21	0.13	0.11	0.05	0.16

Fig. 2. The sensitivity of the structural parameters around their optimum values.
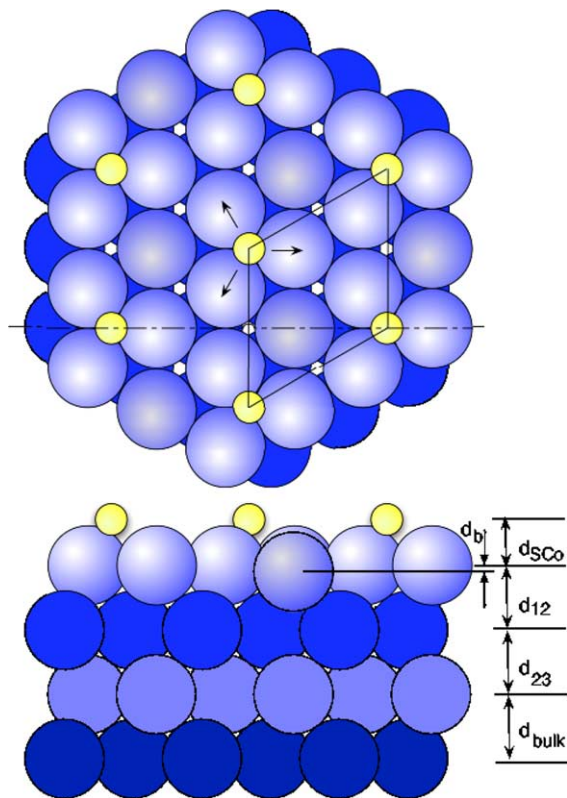

Fig. 3. Top and side views of the optimum (2×2)-S adsorption structure on Co(0001). The numerical values for the structural parameters are given in Table 2.

with experimental relaxations -2.1% and $+1.3\%$ [10] and other theoretical results -3.0% and $+0.6\%$ [26]. The surface energy of the clean Co(0001) surface was also calculated resulting in a value of 2.16 J/m^2 which is larger than the experimental values 1.78–1.87 J/m^2 [27]. This is not a surprise since the surface energy is a sensitive quantity and requires a thick slab to reach saturation. However, the calculated surface energy is about the same as those in other theoretical calculations [26].

For sulfur adsorption on Co(0001) all the high symmetry adsorption sites were calculated. The surface-structure data from these DFT calculations are also shown in Table 2. Due to the S atom on the surface, the interlayer spacing slightly increases between the first and second cobalt layer and decreases between the second and third cobalt layer, compared to the interlayer spacings in the clean Co(0001) surface system. The height of the S atom from the nearest neighbor (NN) Co surface atoms is 1.61 Å while the next-nearest neighbor (NNN) Co surface-layer atoms are a little farther showing buckling d_b of 0.03 Å. The Co–Co distance between the NN Co atoms in the surface layer is increased only by 0.006 Å $(+0.2\%)$ due to S at the fcc hollow site. In the case of S at the hcp site, the S atom is closer to the surface and, thus, the Co–Co distance is increased more, i.e. it is 0.08 Å $(+3.1\%)$ larger than that in the clean Co(0001) surface.

The adsorption energies for sulfur on different adsorption sites on Co(0001) are shown in Table 3. Based on these energies, the most favorable sites are the threefold hollow sites. The difference between the adsorption energies of the fcc and hcp sites is negligible and the barrier for the S atom to jump from the fcc-hollow site to the hcp-hollow site, through the bridge site, is only 0.20 eV. This means that at high temperatures both hollow sites would be occupied.

The similarities in the local density of states (LDOS), shown in Fig. 4, for the case of S atoms at the hollow sites indicate that the nature of bonding between the S atom and Co surface atoms is almost independent of the type of the hollow site. The d-band states for the NNN Co atoms (not shown in Fig. 4) are nearly identical to those for the clean surface Co atoms indicating that the bonding mainly takes place between the S atom and the NN Co surface atoms.

Table 2
The interlayer distances between the Co layers and the height of S atoms at different adsorption sites

		d_{SCo}	d_{12}	d_{23}
LEED	Clean [10]	–	1.99 ± 0.02	2.06 ± 0.02
DFT	Clean	–	1.95	2.03
LEED	S at fcc	1.59 ± 0.06	2.05 ± 0.04	2.03 ± 0.04
DFT	S at fcc	1.61 (1.64)	1.98	2.01
DFT	S at hcp	1.57 (1.60)	1.96	2.02
DFT	S at bridge	1.66 (1.57)	1.98	2.02
DFT	S on top	2.02 (1.87)	1.97	2.02

All distances in Å. There are two calculated interlayer distances between the S atom and the topmost Co layer, namely for the nearest (next-nearest) neighbors. In the bulk, the interlayer distance d_{bulk} between Co layers is 2.01 Å from the DFT calculations. The literature value used also in the LEED experiments is 2.035 Å.

Table 3
Calculated adsorption energies and magnetic moments for the nearest (next-nearest) neighbor Co surface atoms, next to the S atom

	Clean	fcc	hcp	Bridge	Top
E_{ads} (eV)	–	−5.35	−5.33	−5.15	−4.12
μ (μ_B)	1.70	1.46 (1.84)	1.37 (1.78)	1.38 (1.76)	1.23 (1.78)

The magnetic moments of Co atoms in the surface layer are also shown in Table 3. The bulk and surface magnetic moment of Co is $1.66\mu_B$ and $1.70\mu_B$, respectively. Other calculated values for bulk and surface Co atoms are $1.61\mu_B$ and $1.76\mu_B$, respectively [26]. The magnetic moment for the NN Co atom decreases and for the NNN Co atom increases due to S on Co(0001). The magnetic moment of S on the Co(0001) surface is almost zero. The differences in the magnetic properties of Co between the different hollow sites for S are more pronounced than the differences between the corresponding adsorption energies. The larger decrease of the magnetic moment of the NN Co atom as S is located at the hcp site is due to the larger lowering in the spin-up density compared to the case of S at the fcc site (see Fig. 4(a) and (b)).

As one considers the interaction between the Co surface atoms and the S atoms, when S is sitting at the fcc hollow site, one can see in Fig. 5 that the electronic density around the NN Co surface atoms has decreased, seen also in Fig. 4(a) as a lowering in the spin-up states between 0.5 and 2.5 eV below the Fermi level, while there are only minor changes if at all around the other Co atoms in the system. On the other hand, the charge den-sity has increased between the S adatom and the NN Co surface-layer atom. There is also a signifi-cant increase in the electronic density above the S atom, showing a filling of anti-bonding states of S (see also Fig. 4(a) near the Fermi level) that reduces the covalent type of bonding between the Co and S atoms. However, the hybridization between the Co d-states and S p-states is quite strong which can be seen in Fig. 4 between the S spin-up p-states and the Co spin-up d-states around the energies 3, 4 and 5 eV below the Fermi level and also in Fig. 5 between the S and Co atoms (there are three such bonds between the S and the NN Co surface atom because of symme-try). This hybridization explains the large adsorp-tion energy and is thus the reason why S atoms like to sit tightly on the Co surface. The situation is similar to the case of CH$_3$S at the fcc hollow site on Co(0001) [26] showing that the S adatom on the surface can also act as an adsorption site for other atoms and molecules.

4. Discussion

The experimental structure of clean Co(0001) has earlier been published in Ref. [10]. The DFT
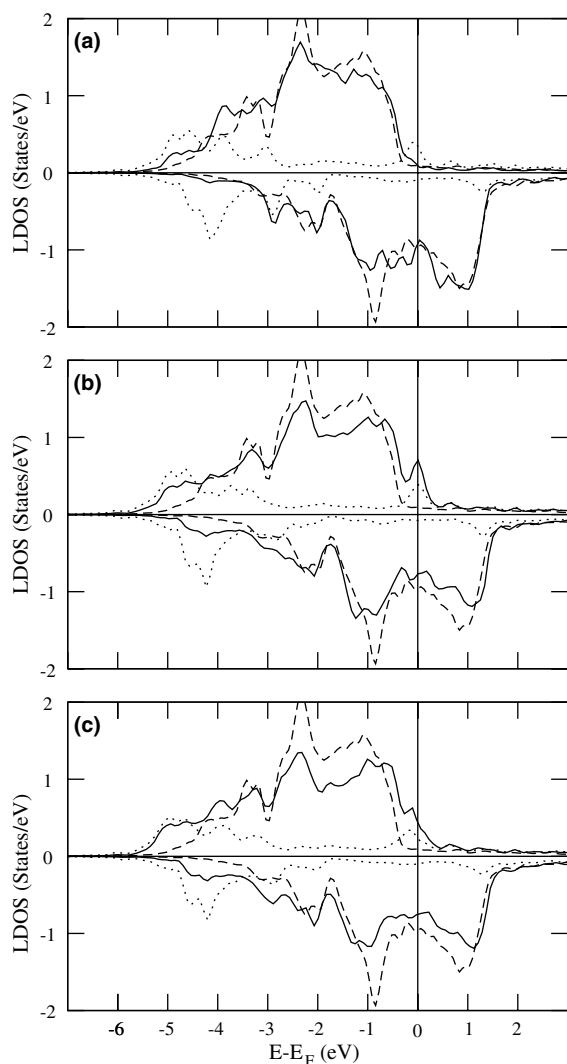
Fig. 4. Local density of spin-up and spin-down states for S on Co(0001) at the (a) fcc, (b) hcp and (c) bridge site: d-band states for the nearest neighbor Co atom from S (solid line), for Co d-band states in the clean Co(0001) surface (dashed line), and p-band states for S (dotted line). E_F is the Fermi energy of the system.

Fig. 5. Changes in the charge density due to S located at the fcc site on Co(0001). The successive contours correspond to ±0.003, ±0.006, ±0.012, ±0.020 electrons $/\text{Å}^3$.

calculations were tested against these values and the comparison is shown in Table 2. The measured and calculated data agree on the (2–3%) inward relaxation of the layer distance between two outermost layers, while the distance between the layers 2 and 3 is extended (1%) compared to the bulk value.

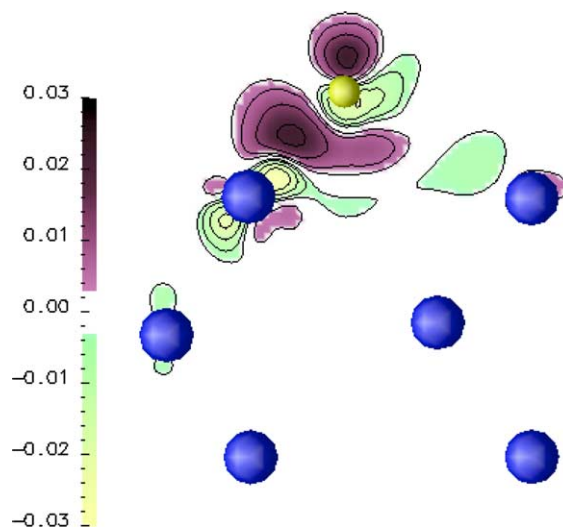A summary of the structural parameters of sulfur on close-packed transition metal surfaces is given in Table 4. Sulfur seems to prefer high coordination sites, on fcc metals the site is fcc-hollow site and on hcp metals the hcp-hollow site, except for Co in which case the fcc-hollow site is preferred.

The interlayer distance between the sulfur atoms and the outermost Co layer is 1.59 ± 0.06 Å from the experimental data, and 1.61 Å from the DFT results. These numbers give 2.19 ± 0.10 Å and 2.16 Å for the experimental and computational S–Co atomic distance, respectively. This distance is smaller than the sulfur–metal bond length of the (2×2)-S structure on Ru(0001) and Re(0001), where the values are 2.29 ± 0.02 Å [4] and 2.32 ± 0.05 Å [5], respectively. With Ni(111)-(2×2)-S structure the sulfur-metal bond length has reported values from 2.11 ± 0.03 Å [6] to 2.23 ± 0.02 Å [7] and they equal with our result on cobalt.

Sulfur is known to form S_n species with S–S bond length of 2.05 Å. Since the S–S bond length on Co(0001) is roughly 5 Å direct chemical bonds between S atoms on the surface are not expected. This finding is also supported by the calculated charge density indicating more local changes in the charge distribution (see Fig. 5).

Table 4
Structural parameters of adsorbed sulfur on metal surfaces

Substrate	Structure	Site	S–S (Å)	S radius (Å)	Buckling (Å)	Method	Refs.
Co(0001)	(2×2)	fcc	2.19	0.94		LEED	This work
Co(0001)	(2×2)	fcc	2.16	0.92	0.03	DFT	This work
Ru(0001)	(2×2)	hcp	2.29	0.94	0.03	LEED	[4]
Re(0001)	(2×2)	hcp	2.32	0.94	0.05	LEED, STM	[5]
Ni(111)	(2×2)	fcc	2.11	0.87		XSW	[6]
Ni(111)	(2×2)	fcc	2.23	0.99		XSW	[7]
Pt(111)	(2×2)	fcc	2.24	0.85		XSW	[8]
Ru(0001)	$(\sqrt{3} \times \sqrt{3})R30°$	hcp	2.28	0.93	–	LEED	[4]
Rh(111)	$(\sqrt{3} \times \sqrt{3})R30°$	fcc	2.23	0.89	–	LEED	[28]
Pd(111)	$(\sqrt{3} \times \sqrt{3})R30°$	fcc	2.20	0.82	–	LEED	[29]
Pt(111)	$(\sqrt{3} \times \sqrt{3})R30°$	fcc	2.25	0.86	–	LEED	[8]
Pt(111)	$(\sqrt{3} \times \sqrt{3})R30°$	fcc	2.28	0.89	–	LEED	[30]
Co(100)	$c(2 \times 2)$	Fourfold	2.20			LEED	[31]

S–S indicates the distance between the sulfur atom and the nearest substrate atom.

The first Co–Co layer distance is experimentally 2.05 ± 0.04 Å and computationally 1.98 Å. Compared with the inward relaxation on clean Co(0001) we can see that the S atoms reduce the inward relaxation, as was reported also with Re(2×2)-S [5]. The second layer distance is almost the same as that with the clean Co(0001) surface.

Our result on the fcc-adsorption site for sulfur is in line with the previous results on several transition metal surfaces showing adsorption at threefold hollow sites. However, the favorable site in the other systems have corresponded with the metal bulk structure. On Ru(0001) [4] and Re(0001) [5] the S adsorption favors the hcp site while on Ni(111) [6] and Pt(111) [8] the fcc site. Based on the DFT results the energy minimum for fcc site is only slightly (0.02 eV) lower than that for the hcp site. This along with the observation of the fairly low energy barrier from the fcc to hcp site through the bridge site (0.20 eV) indicates that adsorption on either site could be possible. The LEED analysis, however, ruled out the hcp site as an experimental result at low temperatures.

The small changes between the threefold hollow adsorption sites can also be read from the changes in the charge density at the surface due to the S adatom, shown in Fig. 5. Thus, it seems that the main interaction takes place between the topmost Co surface atoms and the adsorbed S atoms. The S adatom is tightly bound to the NN Co surface

atom, but there are only small changes in the electronic structure near the other Co atoms, based both on the LDOS and charge density. This points towards interpretation of the poisoning effect of S on Co(0001) as the S atom effectively blocking the site it is located at, but leaving the other sites still active. This can also be seen in experiments [2], where one S atom blocks effectively 1.2 CO sites.

Thus, based on the theoretical results alone it is hard to make any prediction on the preferred adsorption site between the hollow sites, and that is why one should always combine theoretical results with experiments when available. On the other hand, the interpretation of the experimental results can be done more easily if one could lean on some computational results.

5. Conclusions

In this study, we have presented a quantitative structural analysis of the (2×2)-S structure on Co(0001) surface using low-energy electron diffraction together with the dynamical-LEED and DFT calculations.

The favored configuration consists of sulfur atoms residing at the fcc-hollow sites with S–Co distance of 2.19 ± 0.10 Å. Buckling in the first layer is negligible and the three nearest-neighbor Co atoms below the S atom are symmetrically

moved by 0.05 ± 0.09 Å along the surface away from the S atom. The findings are confirmed by the DFT calculations.

Acknowledgements

References

[1] E.L. Hardegree, P. Ho, J.M. White, Surf. Sci. 165 (1986) 488.
[2] K. Habermehl-Cwirzen, J. Lahtinen, Surf. Sci. 573 (2004) 183.
[3] K. Habermehl-Cwirzen, K. Kauraala, J. Lahtinen, Phys. Scr. T108 (2004) 28.
[4] D. Juergens, G. Held, H. Pfnuer, Surf. Sci. 303 (1994) 77.
[5] A. Barbieri, D. Jentz, N. Materer, G. Held, J. Dunphy, D.F. Ogletree, P. Sautet, M. Salmeron, M.A.V. Hove, G.A. Somorjai, Surf. Sci. 312 (1994) 10.
[6] J. Luedecke, A.R.H.F. Ettema, S.M. Driver, G. Scragg, M. Kerkar, D.P. Woodruff, B.C.C. Cowie, R.G. Jones, S. Bastow, Surf. Sci. 366 (1996) 260.
[7] D.R. Warburton, P.L. Wincott, G. Thornton, F.M. Quinn, D. Norman, Surf. Sci. 211/212 (1989) 71.
[8] H.A. Yoon, N. Materer, M. Salmeron, M.A.V. Hove, G.A. Somorjai, Surf. Sci. 376 (1977) 254.
[9] J. Lahtinen, J. Vaari, K. Kauraala, E.A. Soares, M.A. VanHove, Surf. Sci. 448 (2000) 269.
[10] J. Lahtinen, J. Vaari, T. Vaara, P. Kaukasoina, M. Lindroos, Surf. Sci. 425 (1999) 90.
[11] J. Lahtinen, K. Kauraala, J. Vaari, T. Vaara, P. Kaukasoina, M. Lindroos, Phys. Rev. B 63 (2001) 155402.
[12] K. Pussi, M. Lindroos, J. Katainen, K. Habermehl-Cwirzen, J. Lahtinen, A.P. Seitsonen, Surf. Sci. 572 (2004) 1.
[13] J. Lahtinen, J. Vaari, A. Talo, A. Vehanen, P. Hautojärvi, Vacuum 41 (1990) 112.
[14] J. Lahtinen, J. Vaari, A. Talo, A. Vehanen, P. Hautojärvi, Surf. Sci. 245 (1991) 244.
[15] T. Vaara, J. Vaari, J. Lahtinen, Surf. Sci. 395 (1998) 88.
[16] A. Barbieri, M.A. VanHove, Private communication.
[17] J.B. Pendry, J. Phys. C 13 (1980) 937.
[18] G. Kresse, J. Hafner, Phys. Rev. B 47 (1993) 558.
[19] G. Kresse, J. Furthmüller, Comput. Mater. Sci. 6 (1996) 15.
[20] G. Kresse, J. Furthmüller, Phys. Rev. B 54 (1996) 11169.
[21] P.E. Blöchl, Phys. Rev. B 50 (1994) 17953.
[22] G. Kresse, J. Joubert, Phys. Rev. B 59 (1999) 1758.
[23] J.P. Perdew, in: P. Ziesche, H. Eschrig (Eds.), Electronic Structure of Solids '91, Academic Verlag, Berlin, 1991.
[24] H.J. Monkhorst, J.D. Pack, Phys. Rev. B 13 (1976) 5188.
[25] WebElements, the periodic table on the WWW, URL: http://www.webelements.com, Copyright 1993–2005 Mark Winter [The University of Sheffield and WebElements Ltd., UK].
[26] L.G. Wang, E.Y. Tsymbal, S.S. Jaswal, Phys. Rev. B 70 (2004) 075410.
[27] C.T. Lynch (Ed.), CRC Handbook of Materials Science, General Properties, Vol. I, CRC Press Inc., Boca Raton, Florida, 1974, p. 107.
[28] K.C. Wong, W. Liu, M. Saidy, K.A.R. Mitchell, Surf. Sci. 345 (1996) 101.
[29] M.E. Grillo, C. Stampfl, W. Berndt, Surf. Sci. 317 (1994) 84.
[30] K. Hayek, H. Glassl, A. Gutmann, H. Leonhard, M. Prutton, S.P. Tear, M.R. Welton-Cook, Surf. Sci. 152/153 (1985) 419.
[31] M. Maglietta, Solid State Commun. 43 (1982) 395.